

Kent Academic Repository

Full text document (pdf)

Citation for published version

Zhang, Qian and Mahfouf, Mahdi and Yates, John R. and Pinna, Christophe and Panoutsos, George and Boumaiza, Soufiene and Greene, Richard J. and de Leon, Luis (2011) Modeling and Optimal Design of Machining-Induced Residual Stresses in Aluminium Alloys Using a Fast Hierarchical Multiobjective Optimization Algorithm. *Materials and Manufacturing Processes*, 26 (3). pp.

DOI

<https://doi.org/10.1080/10426914.2010.537421>

Link to record in KAR

<https://kar.kent.ac.uk/50508/>

Document Version

Pre-print

Copyright & reuse

Content in the Kent Academic Repository is made available for research purposes. Unless otherwise stated all content is protected by copyright and in the absence of an open licence (eg Creative Commons), permissions for further reuse of content should be sought from the publisher, author or other copyright holder.

Versions of research

The version in the Kent Academic Repository may differ from the final published version.

Users are advised to check <http://kar.kent.ac.uk> for the status of the paper. **Users should always cite the published version of record.**

Enquiries

For any further enquiries regarding the licence status of this document, please contact:

researchsupport@kent.ac.uk

If you believe this document infringes copyright then please contact the KAR admin team with the take-down information provided at <http://kar.kent.ac.uk/contact.html>

Modelling and optimal design of machining induced residual stresses in aluminium alloys using a fast hierarchical multi-objective optimisation algorithm

Qian Zhang^a, Mahdi Mahfouf^a, John R. Yates^b, Christophe Pinna^b, George Panoutsos^a, Soufiene Boumaiza^b, Richard J. Greene^b, Luis de Leon^c

^aDepartment of Automatic Control and Systems Engineering, The University of Sheffield, Sheffield, S1 3JD, UK. E-mail: {qian.zhang, m.mahfouf, g.panoutsos}@sheffield.ac.uk

^bDepartment of Mechanical Engineering, The University of Sheffield, Sheffield, S1 3JD, UK. E-mail: {j.yates, c.pinna, s.boumaiza, r.j.greene}@sheffield.ac.uk

^cInstitute of Production Engineering and Machine Tools, Leibniz University, Hannover, Germany. E-mail: leon@ifw.uni-hannover.de

Abstract

The residual stresses induced during shaping and machining play an important role in determining the integrity and durability of metal components. An important issue of producing safety critical components is to find the machining parameters that create compressive surface stresses or minimise tensile surface stresses. In this paper, a systematic data-driven fuzzy modelling methodology is proposed, which allows constructing transparent fuzzy models considering both accuracy and interpretability attributes of fuzzy systems. The new method employs a hierarchical optimisation structure to improve the modelling efficiency, where two learning mechanisms cooperate together: NSGA-II is used to improve the model's structure while the gradient descent method is used to optimise the numerical parameters. This hybrid approach is then successfully applied to the problem that concerns the prediction of machining induced residual stresses in aerospace aluminium alloys. Based on the developed reliable prediction models, NSGA-II is further applied to the multi-objective optimal design of aluminium alloys in a 'reverse-engineering' fashion. It is revealed that the optimal machining regimes to minimise the residual stress and the machining cost simultaneously can be successfully located.

1. Introduction

In material engineering and mechanical engineering, residual stresses (or secondary stresses) play an important role in the integrity of a structure [1]. Their combination with primary loads contributes to changes in the operating performance of mechanical parts. Tensile residual stresses enhance the likelihood of fatigue, fracture and corrosion induced failures. Conversely, compressive residual stresses are often introduced by shot-peening and burnishing to enhance structural integrity and durability [2].

Metal removal by machining operations such as milling and drilling induces residual

stresses in the near surface region. These stresses are highly dependent on the machining parameters and cannot be accurately described using mathematical models because of the high complexity of the processes. Finite Element Methods (FEMs) have been widely used to investigate this phenomenon [3]. The drawbacks of FEM approaches relate to the long time needed for the solution of complex models and their inability to learn from examples. In recent years, some intelligent data-driven modelling approaches have been considered for the prediction of residual stresses. For instance, Artificial Neural Networks (ANNs) have been used by Kafkas *et al.* [4] and Umbrello *et al.* [5].

In this paper, a systematic data-driven modelling methodology, based on fuzzy systems, is proposed to model machining induced residual stresses. Compared with analytically based methods, such as FEMs, fuzzy systems are simpler in structure and easier to apply. They are capable of learning from data without needing much prior knowledge about the materials and machining processes. Fuzzy models are also convenient when combined with optimisation techniques to identify the input parameters that will provide a desirable residual stress profile. On the other hand, compared with black-box modelling approaches, such as ANNs, fuzzy systems have transparent characteristics and the relationships between inputs and outputs are more interpretable, because of their use of descriptive language, such as linguistic ‘IF-THEN’ rules.

The proposed fuzzy modelling methodology allows to generate fuzzy models considering not only accuracy (precision) but also transparency (interpretability) of fuzzy systems via applying multi-objective optimisation techniques. As a result, a set of so-called ‘Pareto-optimal’ [6] models, in terms of different accuracy and interpretability levels, are constructed, which provide a wide range of choices for practitioners or users. In the previously proposed modelling strategy [7, 8], all the elements relating to the models, both the structure and parameters, were included in the multi-objective optimisation scheme. This method met some level of difficulty when dealing with high-dimensional problems, where hundreds of decision variables may need to be optimised simultaneously. In this paper, a hierarchical optimisation structure is proposed to improve the modelling efficiency, where two learning methods are systematically combined in order to improve various attributes of fuzzy systems: One multi-objective optimisation algorithm, the Non-dominated Sorting Genetic Algorithm II (NSGA-II) [9], is used to optimise the model’s structure; Based on a fixed model structure, the other single-objective learning paradigm, the Gradient Descent (GD) method is employed to improve the model’s parameters.

Once the prediction models of residual stresses are successfully elicited, they are further exploited for multi-objective optimal design of aluminium alloys, which aims at determining the optimal machining regime(s) to obtain the desired residual stress profile while minimising the machining cost. For this application, the NSGA-II is used again to produce a range of well-spread Pareto-optimal solutions, which have

little residual stresses while maintaining reasonable production costs.

This paper is organised as follows. Section 2 introduces the details about the related material and manufacturing process. Section 3 describes the details of the proposed modelling framework. In Section 4, the experimental studies for modelling the machining induced residual stresses in aluminium alloys are presented. In Section 5, the experiments relating to the multi-objective optimal design of aluminium alloys are conducted. Finally, concluding remarks are given in Section 6.

2. The COMPACT project and machining induced residual stresses

Part distortion is a function of residual stress and is caused by the complex combination of material processing, or the complex interaction between material processing. In aerospace industry, excessive distortion may result in the rejection of a part as well as costly and time-consuming rework before placement in service. It is reported that tens of millions of Euros are spent every year in an attempt to either avoid or remedy distortion in components [10].

COMPACT (COncurrent approach for Manufacturing induced Part distortion in Aerospace ComponenTs) is a research programme that proposes to investigate manufacturing induced part distortion in aerospace alloy components. This project was funded by the European Union under the Framework 6 initiative, led by Airbus UK and included 12 industrial and academic partners from across Europe. The University of Sheffield focused on the simulation and prediction of part distortion of residually stressed parts using finite element modelling combined with a systems modelling approach.

As an example, the following shows various phases of a part fabrication process as well as the related modelling simulation.

1. **Material preparation:** A billet of the aluminium alloy Al7449 was obtained through a rolling process. In this case, a rectangular section of the billet, from which a component is to be fabricated, is considered. The geometry is shown in Figure 1, where the relevant axes are defined as: 1 – transverse rolling direction (LT); 2 – through-thickness direction (ST); 3 – rolling direction (L).
2. **Machining:** Some material was removed from this rectangular section using a milling machine to form a multi-channel specimen consisting of three linear channels. To simulate the removal of material and the effect due to machining efforts, thermal effects and the contact with cutting tool, the FEM method needs the profile of the surface and near-surface machining induced residual stresses. The prediction of the machining induced residual stresses was conducted using the systems modelling approach introduced in this paper, where the training data for the prediction models were measured using a X-ray diffraction technique by the University of Hannover [11].

3. Part distortion due to material removal: After the machining operation, the work piece was unclamped, which means that the component is free to relax and is allowed to distort and attain its final equilibrium state. Figure 2 shows the predicted distortion under residual stresses [12].

Besides the above instance, other specimens with different geometries were also studied, such as those shown in Figure 3. In the following sections, the systems modelling approach, which was employed in the prediction of machining induced residual stresses (Step 2 of last paragraph), as well as the relevant experiments, will be introduced in detail.

3. The proposed hierarchical multi-objective fuzzy modelling approach

3.1 Introduction to fuzzy systems

Fuzzy rule-based systems are viewed as robust ‘universal approximators’ [13] capable of performing nonlinear mappings between inputs and outputs. It is an approach that allows a system to be represented using a descriptive language (linguistic ‘IF-THEN’ rules), which can easily be understood and explained by humans to allow them to gain a deeper insight into uncertain, complex and ill-defined systems.

Generally, a fuzzy system consists of four fundamental components: fuzzy rule-base, fuzzy inference engine, fuzzifier and defuzzifier. Figure 4 shows the diagram of a fuzzy system. The central part of a fuzzy system is the knowledge-base (rule-base) consisting of the fuzzy rules. A fuzzy rule is an IF-THEN statement in which some words are characterised by continuous membership functions. Specifically, the fuzzy rule-base comprises the following fuzzy rules:

Rule_{*l*}: IF x_1 is A_1^l AND ... AND x_n is A_n^l , THEN y is B^l ,
 where $l = 1, 2, \dots, m$; m is the number of rules in the fuzzy rule-base; A_i^l and B^l are fuzzy sets in $U_i \subset R$ and $V \subset R$, respectively, and $\mathbf{x} = (x_1, x_2, \dots, x_n)^T \in U$ and $y \in V$ are the input and output (linguistic) variables of the fuzzy system, respectively.

The fuzzifier is defined as a mapping from a real-valued point $x^* \in U \subset R^n$ to a fuzzy set A^* in U . Normally, three types of fuzzifiers are used, which are singleton fuzzifier, Gaussian fuzzifier and triangular fuzzifier. They correspond to three types of fuzzy sets with different shapes of membership functions. In a fuzzy inference engine, fuzzy logic principles direct how to employ the fuzzy rules into a mapping from an input fuzzy set A^* to an output fuzzy set B^* . The defuzzifier is a mapping from the output fuzzy set B^* in $V \subset R$ to a real-valued point $y^* \in V$. Conceptually, the purpose of the defuzzifier is to specify a point in V that best represents B^* . Three widely used defuzzifiers are centre of gravity defuzzifier, centre average defuzzifier and maximum defuzzifier. For more details about fuzzy systems, please refer to [14].

Fuzzy modelling is a systems modelling approach with fuzzy rule-based systems. In

most of the fuzzy modelling methods, the fuzzy inference engine and the defuzzifier are predefined. Thus, the primary work is to generate appropriate fuzzy sets and right fuzzy rules.

3.2 A fast hierarchical multi-objective fuzzy modelling approach

Generally, data-driven fuzzy modelling can be viewed as a two-step process. The first step aims to generate a ‘crude’ approximation of the fuzzy model. The second step consists of optimising the initial fuzzy rules and fuzzy sets to lead to a final ‘optimised’ fuzzy model.

For the first step, it can be achieved via two different methods: the grid-partitioning based method or the clustering based method. For the first method, the grid-partitioning defines a number of evenly distributed fuzzy sets for each variable. These fuzzy sets are shared by all the fuzzy rules. The big disadvantage of this method is its huge number of fuzzy rules for high-dimensional modelling problem. In contrast, the second method employs data clustering information to define fuzzy sets. The fuzzy sets are not shared by all the rules, but each set is only mapped into one particular fuzzy rule. In this method, each fuzzy rule is associated to one cluster. In this paper, the clustering based method is employed, which includes a previously developed high-performance clustering algorithm, an agglomerative complete-link clustering algorithm [15].

For the second step, the main learning and optimisation techniques include linear least squares, gradient descent methods, neuro-fuzzy training methods, and some evolutionary optimisation techniques (evolutionary fuzzy systems). Compared with the fuzzy systems using other learning techniques, evolutionary fuzzy systems are able to realise improvements on not only the parameters but also the structure of the fuzzy systems. Moreover, multi-objective optimisation techniques within the evolutionary computation can prove very helpful in studying the trade-off between the accuracy and the interpretability of fuzzy systems. Some recent works in the literature [16; 17] have employed multi-objective optimisation techniques to tackle the trade-off issue of fuzzy models. But most of them were carried out based on grid-partitioning-type fuzzy sets and cannot avoid the difficulty associated with the curse of dimensionality.

In the previously proposed modelling approach [7, 15], a multi-objective optimisation algorithm was used to improve fuzzy models’ structure and tune their parameters at the same time. This method would use relatively more calculation and would take longer to converge when dealing with high-dimensional modelling problems, where a large number of decision variables need to be adjusted and optimised simultaneously.

In this paper, a hierarchical optimisation structure is proposed, where two learning techniques conduct sequentially and iteratively to improve the different aspects of

fuzzy systems: the multi-objective optimisation algorithm NSGA-II [9] is mainly employed to optimise the model's structure; while the gradient descent method is employed to improve the model's parameters. The NSGA-II algorithm has been demonstrated as one of the most efficient algorithms for multi-objective optimisation on a number of benchmark problems and applications. Two of the most important features in NSGA-II lie in its fast non-dominated sorting procedure and an elitist strategy. The detailed implementation procedure can be found in [9]. Gradient descent is a first-order optimisation algorithm that can quickly find a local minimum of a function. It has widely been employed in fuzzy modelling for tuning the membership functions [14] and shown to perform efficiently in improving the accuracy of fuzzy models.

Figure 5 illustrates the proposed fuzzy modelling approach. This approach will be referred to throughout as a Fast Hierarchical Multi-Objective Fuzzy Modelling (FHMO-FM) approach. It can be divided into several components and the execution steps can be described as follows:

1. **Data clustering:** A modified agglomerative complete-link clustering algorithm [15] is employed to process training data in order to obtain the information relating to clusters. This algorithm has been shown to be more efficient and perform better than other well-known clustering algorithms, such as the fuzzy c-means (FCM) clustering algorithm [8].
2. **Initial model construction:** The information that these clusters provide is then used to construct an initial fuzzy model. In this approach, one cluster corresponds directly to one fuzzy rule; the centres of membership functions are defined using the information of their corresponding clusters' centre positions; other parameters relating to the membership functions are defined under the principle that one membership function must cover all the training data, which are included in its corresponding cluster. More details about this step have been introduced in [7].
3. **Interpretability improvement:** The fuzzy system is improved in structure, including the variation of the fuzzy rules and fuzzy sets, considering the interpretability issue. This task can be achieved using a four-step operation, including (1) removing redundant fuzzy rules, (2) merging similar fuzzy rules, (3) removing redundant fuzzy sets and (4) merging similar fuzzy sets. These four steps are controlled by 4 threshold parameters, $Th_1 - Th_4$. The details relating to the whole operation have been explained in [15].
4. **Accuracy improvement:** The fuzzy models are improved by the gradient descent method [14] in terms of accuracy based on a fixed modelling structure.
5. **Non-dominated sorting and crowed sorting:** The non-dominated fuzzy models with a good diversity are found using the non-dominated sorting and crowed sorting mechanism, which are introduced in the algorithm NSGA-II [9].
6. **Termination check:** If the termination criterion is achieved, the modelling process is stopped and the final Pareto-optimal solutions are obtained; if not, all the modelling and performance information are passed to the algorithm NSGA-II. Normally, the termination criteria are designed so that the number of function

evaluations achieves a predefined value.

7. **Multi-objective optimisation using NSGA-II:** The algorithm generates new control parameters ($Th_1 - Th_4$) for interpretability improvement based on the multi-objective optimisation strategy, then return to Step 3. It should be noted that the structure of a fuzzy model is not directly coded into the optimisation procedure, but is rather varied and optimised via controlling the thresholds. The accuracy of a fuzzy model can be evaluated using the Root Mean Square Error (RMSE) index, which is described as follows:

$$RMSE = \sqrt{\frac{\sum_{l=1}^N (y_l^m - y_l^p)^2}{N}} \quad (1)$$

where y_l^m is the measured output data and y_l^p is the predicted output data, $l = 1, 2, \dots, N$; N is the total number of data. The interpretability of a fuzzy model is affected by the number of fuzzy rules ($Nrule$), the number of fuzzy sets ($Nset$) and the total length of fuzzy rules ($Lrule$). To normalise these two objectives and make them similar and comparable in scale, they are formulated as follows:

$$\begin{aligned} \text{Objective 1: } & \frac{RMSE}{RMSE_l} \\ \text{Objective 2: } & \frac{Nrule}{Nrule_l} + \frac{Nset}{Nset_l} + \frac{Lrule}{Lrule_l} \end{aligned} \quad (2)$$

where $RMSE_l$ is the root mean square error of the fuzzy model that is not optimised using the multi-objective optimisation mechanism; $Nrule_l$, $Nset_l$ and $Lrule_l$ represent the number of fuzzy rules, the number of fuzzy sets and the total rule length of this fuzzy model, respectively.

4. Experimental results of modelling residual stresses

Residual stress is that stress which remains in a material body that is stationary and at equilibrium with its surroundings [18]. Normally, residual stresses originate from thermal or elastic misfits either between different regions or between different phases within a material [18], caused by heat treatment, machining, welding or combinations thereof. Residual stress can be very detrimental to the performance of a material or the life of a component, since it may [19]:

- Induce premature failure through cracking
 - Reduce fatigue strength
- Induce stress corrosion or hydrogen cracking
- Cause distortion and dimensional variation

Under the framework of the COMPACT project, the multi-objective evolutionary algorithm NSGA-II is implemented into the systems modelling of machining induced residual stresses. In materials science and engineering, similar ideas have been widely explored. For example, Evolutionary Strategy (ES) has been employed to assess the coefficients of the Barlat yield criterion for anisotropic alloy sheets [20] and Particle Swarm Optimisation (PSO) has been applied to the optimal design of the mechanical properties of alloy steels [21] (For more state of the art information about the applications of evolutionary algorithms and multi-objective optimisation techniques in the area of materials processing, refer to the following two review articles [22, 6]).

Extensive experimental tests relating to the machining induced surface residual stresses in aluminium alloys have been conducted by the Institute of Production Engineering and Machine Tools (IFW), the

University of Hannover. These surface and near-surface residual stresses (up to 250 μm in depth) in aerospace aluminium parts were obtained using the X-ray diffraction measurements and include the profiles of a wide range of machining parameters, such as cutting tool geometry, cutting speed, feed velocity, feed per tooth etc. Two typical sets of such residual stress measurements are used in the following modelling experiments, which includes 5 and 13 input variables, respectively.

4.1 Experiment 1: the 5-dimensional modelling problem

In the first case, 207 residual stress data were used for training and 36 data were used for final testing. System inputs include cutting speed, feed per tooth, feed velocity, coolant medium and measurement depth. The residual stress in the longitudinal rolling direction of the original aluminium billet is the modelling target.

In this experiment, the initial fuzzy model was obtained using 15 clusters, resulting in a model with 15 rules and 90 fuzzy sets. For the NSGA-II algorithm, the population size and the archive size were set to be 50 and the number of generation was set to be 200, all other parameter settings were as same as those in [9].

The experiment was carried out over 20 runs. One set of results out of the 20 runs is randomly selected and shown in the following paragraphs. Figure 6 demonstrates the trade-offs among the Pareto-optimal models respect to the multiple objectives and various criteria, including the RMSE, the number of fuzzy rules, the number of fuzzy sets and the total length of fuzzy rules.

Table 1 includes the main parameters of the initial model as well as three optimised fuzzy models, which are selected from all the Pareto-optimal models and with 15, 14 and 12 rules respectively. Figure 7 shows the prediction performance of these models. It can be seen that, for these optimised models, more rules and more parameters will bring more accuracy while the models with fewer rules and parameters are simpler in structure and easier to understand.

To provide more details about the obtained fuzzy models, Figure 8 shows an example of two fuzzy rules out of the rule-base for the optimised 14-rule model. For these fuzzy rules, they can be rewritten as the following approximate linguistic rules using the linguistic hedges approach [23]:
 Rule R_5 : IF Feed per Tooth is *more or less medium large* AND Coolant is *the first type (dry)* AND Test Depth is *medium small*, THEN Residual Stress is *medium small*.
 Rule R_{14} : IF Cutting Speed is *more or less medium small* AND Feed Velocity is *more or less medium small* AND Coolant is *the second type (emulsion)* AND Test Depth is *quite medium small*, THEN Residual Stress is *small*.

By using the generated models, the residual stress curves can also be obtained. They are achieved by plotting one input variable, measurement depth, against the output, residual stress, while keeping other input variables constant. Figure 9 shows both the predicted and the measured residual stress curves based on the testing data, where the predicted curves were elicited using the optimised 15-rule model. It can be seen that the obtained model can predict the residual stress very accurately.

To verify the physical interpretation of the obtained model, Figure 10 shows two three-dimensional response surfaces of the obtained 15-rule residual stress model. These surfaces are achieved by plotting two varying input variables against the output while keeping other input variables constant. From the first surface, it can be seen that, with increasing measurement depth, the absolute value of the residual stress is first increasing and then decreasing. This trend is consistent with the expected behaviour as predicted by the knowledge experts.

4.2 Experiment 2: the 13-dimensional modelling problem

In the second modelling problem, 265 residual stress data were used for training and 19 data were used for testing. There are 13 system inputs in total, which are rotational speed, feed per tooth, feed velocity, width of cut, measurement depth as well as

geometry information about the machining tool: clearance angle flank, rake angle flank, helix angle, width of chamfer flank, clearance angle end, axial angle, width of chamfer end and tool corner radius. In this experiment, the initial number of clusters was set to 15, which means that the initial fuzzy model was generated using 15 rules. For NSGA-II, the configuration of all the parameters was set the same as those used in Section 4.1.

The experiment was repeated 20 times. One set of models out of the 20 runs is randomly chosen and discussed next. Figure 11 demonstrates the trade-offs among the multiple objectives and criteria within 50 Pareto-optimal fuzzy models. Table 2 includes the main parameters of the initial model and three selected optimised models, which are with 15, 13 and 12 rules respectively. Figure 12 shows the prediction performance of these models. It can be observed that these Pareto-optimal models exhibit fuzzy sets pattern behaviour, which means that they provide a wider choice of different solutions to users.

To provide more details about the obtained fuzzy models, Figure 13 shows two fuzzy rules out of the rule-base of the optimised 13-rule model. For these fuzzy rules, the linguistic hedges approach [23] can be employed to derive linguistic rules of the following form:

Rule R_9 : IF Rotational Speed is *large* AND Feed per Tooth is *medium small* AND Feed Velocity is *medium small* AND Rake Angle Flank is *medium small* AND Width of Chamfer Flank is *medium large* AND Axial Angle is *medium small* AND Width of Chamfer End is *medium small* AND Tool Corner Radius is *very small* AND Width of Cut is *more or less medium large* AND Test Depth is *medium small*, THEN Residual Stress is *medium small*.

Rule R_{10} : IF Rotational Speed is *large* AND Feed per Tooth *medium* AND Feed Velocity is *medium* AND Clearance Angle Flank is *medium large* AND Rake Angle Flank is *more or less medium large* AND Helix Angle is *large* AND Clearance Angle End is *more or less medium large* AND Axial Angle is *very small* AND Tool Corner Radius is *very small* AND Width of Cut is *medium* AND Test Depth is *more or less medium small*, THEN Residual Stress is *medium*.

Based on such obtained fuzzy models, the residual stress curves as a function of depth below the machined surface can be generated. Figure 14 compares the measured residual stress curves with the ones that are predicted by the optimised 15-rule model. It can be seen that the fuzzy models can predict the shape and the trend of the experimental residual stress curves very well.

Figure 15 shows two three-dimensional response surfaces for the obtained 15-rule residual stress models. From the first surface, it can be seen that, with an increasing feed velocity, the absolute value of the residual stress tends to increase. This behaviour is consistent with the one which would have been predicted by 'experts'. It is also worth noting that this fuzzy model represents a nonlinear mapping with a good generalisation ability, which is evidenced by the smooth input-output response surface.

5. Optimal design of aluminium alloys

After the accurate and reliable prediction models have been developed, they can be further applied to facilitate the optimal design of aluminium alloys for achieving the overarching aim of 'right-first-time production' of metals [24] as a stand-alone application. Figure 16 illustrates the strategy how to exploit a prediction model in a 'reverse-engineering' fashion to identify optimal recipes for system design.

In recent years, multi-objective optimisation techniques have been applied to the design of alloys, including steels [25], superalloys [26], bulk metallic glasses [27], based on the developed intelligent models. In this work, NSGA-II was further applied to the optimal design, which aims to find the optimal machining regime to minimising

the residual stress in the aluminium alloy while minimising the machining cost. The paradigm and obtained solutions may further be used in controlling the real machining operations.

Based on the analysis in [28], the main cost of a machined piece is the sum of two costs:

$$C_U = C_L + C_T \quad (3)$$

where C_U is the total unit (per piece) cost, C_L is the labour cost per piece and C_T is the tool cost per piece. The labour cost per piece can be expressed as follows:

$$C_L = K_L t_m = K_L \frac{L}{x_{FV}} \quad (4)$$

where K_L is the total labour cost per unit time, t_m is the machining time per piece, L is the length of cut, and x_{FV} represents the feed velocity. The tool cost per piece can be expressed as follows:

$$C_T = K_T \frac{t_m}{t} = K_T \frac{L}{x_{FV} t} \quad (5)$$

where K_T is the cost of a cutting edge, t is the tool life for the cutting edge, and t_m/t means the number of tool consumed per piece.

The Taylor equation for tool life can be written as follows:

$$x_{CS} t^n = K \quad (6)$$

where x_{CS} represents the cutting speed; n and K are constants for a certain cutting tool. Thus, the total unit cost can be rewritten as follows:

$$C_U = C_L + C_T = K_L \frac{L}{x_{FV}} + K_T \frac{L x_{CS}^{1/n}}{x_{FV} K^{1/n}}. \quad (7)$$

To describe the surface and near surface residual stress of a machined piece precisely, the average value of the residual stresses at various test depths (up to 250 μm) is considered. It can be expressed as follows:

$$J = \frac{\sum_{i=1}^{10} |f_{FS}(x_{CS}, x_{FT}, x_{FV}, x_{CM}, x_{MD}(i) = 25i)|}{10} \quad (8)$$

where $f_{FS}()$ represents the output of the residual stress model; x_{CS} , x_{FT} , x_{FV} , x_{CM} , x_{MD} are the input variables of this model, relating to cutting speed, feed per tooth, feed velocity, coolant medium and measurement depth, respectively.

In the following, two experiments were conducted based on the previously developed model, which is the optimised 15-fule fuzzy model introduced in Section 4.1. For the optimisation tool NSGA-II, the population size was set to be 50 and the number of generation was set to be 500, all other parameter settings followed the experiments in [9]. The factors contributing to the machining cost are summarised in Table 3, which are approximate values without any loss of generality.

5.1 Experiment 1

In this experiment, the decision variable is cutting speed. The feed per tooth was set to be a constant value 0.2 and the coolant medium was fixed to be ‘emulsion’. For feed velocity, it can be expressed using the following equation

$$x_{FV} = n_t x_{FT} \frac{x_{CS}}{\pi D} \quad (9)$$

where n_t is the number of teeth ($n_t = 4$ in all the following experiments), x_{FT} represents the feed per tooth, and D is the tool diameter ($D = 63\text{mm}$ in all the following experiments). As $x_{FT} = 0.2$ in this case, Equation (9) can be written as

$$x_{FV} = 4.0441x_{CS}. \quad (10)$$

Thus, two objective functions can be designed as follows:

$$\text{Minimise } J_1 = \frac{\sum_{i=1}^{10} |f_{FS}(x_{CS}, x_{FT} = 0.2, x_{FV} = 4.0441x_{CS}, x_{CM} = 2, x_{MD}(i) = 25i)|}{10}$$

$$\text{Minimise } J_2 = K_L \frac{L}{4.0441x_{CS}} + K_T \frac{Lx_{CS}^{1/n-1}}{4.0441K^{1/n}} \quad (11)$$

where J_1 and J_2 represent the mean absolute residual stress and the machining cost, respectively.

The optimisation experiment was carried out in multiple runs and very consistent and similar results were obtained in different runs. Figure 17 shows one set of the obtained Pareto-optimal solutions in the objective space. Ten various solutions are selected from the Pareto-optimal solutions and listed in Table 4. For those users who tend to prioritise ‘quality’ more, they could choose a design with lower residual stress. For those users who are more concerned with production cost, they may choose a design with lower machining cost. Finally, for those users who have no preference between quality and cost, a ‘median’ design may be the suitable choice.

5.2 Experiment 2

In this case, the decision variables consist of cutting speed, feed per tooth and coolant medium. Based on Equation (9), the feed velocity can be written as follows:

$$x_{FV} = 20.220x_{FT}x_{CS} \quad (12)$$

when $n_t = 4$ and $D = 63\text{mm}$.

Two objective functions in this experiment are designed as follows:

$$\text{Minimise } J_1 = \frac{\sum_{i=1}^{10} |f_{FS}(x_{CS}, x_{FT}, x_{FV} = 20.220x_{FT}x_{CS}, x_{CM}, x_{MD}(i) = 25i)|}{10}$$

$$\text{Minimise } J_2 = K_L \frac{L}{20.220x_{FT}x_{CS}} + K_T \frac{Lx_{CS}^{1/n-1}}{20.220x_{FT}K^{1/n}} \quad (13)$$

where J_1 and J_2 represent the mean absolute residual stress and the machining cost, respectively.

This optimisation experiment was repeated for multiple runs and very consistent results were obtained. One set of the obtained Pareto-optimal solutions is shown in Figure 18. Ten different solutions are selected and their details are provided in Table 5. From this latter table, it can be observed that the generated solutions are consistent with our understanding about the relevant system in its physical and economic behaviours. For instance, a high cutting speed normally brings more residual stress. For a solution with a high cutting speed and a large value of feed per tooth, the feed velocity should be very high. This shortens the machining time for a single component, and therefore decreases its machining costs, and as a result also labour costs.

From the above two experiments, it can be seen that, for the optimal design problems that consider both the machining quality and the economical factor, NSGA-II is able to obtain a set of optional solutions (Pareto-optimal solutions), which provide various levels of residual stress profiles and machining costs.

6. Conclusions

Residual stresses are very essential in determining the integrity and durability of metal components. To simulate the manufacturing induced part distortion in aerospace alloy components, a systems-modelling approach has been developed and employed to predict the machining induced residual stresses. In this paper, a systems modelling framework, named FHMO-FM, has been proposed, where the multi-objective optimisation technique has been employed to improve both the accuracy and the interpretability attributes of fuzzy models, and a hierarchical optimisation structure, including two learning techniques (NSGA-II and gradient descent), has also been included to improve the modelling efficiency. As a result, the proposed approach has been successfully applied to the prediction of the machining induced residual stresses in aerospace aluminium alloys. The physical interpretation of the obtained models has been shown to be consistent with the expected behaviour as predicted by theory and by knowledge experts. Furthermore, the elicited models have been successfully exploited in a ‘reverse-engineering’ fashion via the multi-objective optimal design of aluminium alloys, which aims at determining the optimal machining regimes to minimise the residual stress by taking into account economical factors. Simulation results have shown that NSGA-II is able to produce a range of well-spread optional solutions with low residual stresses while maintaining reasonable production costs.

Acknowledgements

The authors wish to thank the anonymous reviewers for their comments which helped to improve the quality of this paper. They also wish to acknowledge the financial support for this work from the European Union under the Framework 6 initiative.

References:

- [1] British Energy Generation Ltd. Assessment of the Integrity of Structures Containing Defects, R6 Revision 4, 2006.
- [2] McClung, R.C. A Literature Survey on the Stability and Significance of Residual Stresses during Fatigue. *Fatigue and Fracture of Engineering Materials and Structures* **2007**, 30, 173-205.
- [3] Ee, K.C.; Dillon Jr., O.W.; Jawahir, I.S. Finite Element Modeling of Residual Stresses in Machining Induced by Cutting using a Tool with Finite Edge Radius. *International Journal of Mechanical Sciences* **2005**, 47, 1611-1628.
- [4] Kafkas, F.; Karatas, C.; Sozen, A.; Arcaklioglu, E.; Saritas, S. Determination of Residual Stresses based on Heat Treatment Conditions and Densities on a Hybrid (FLN2-44-5) Powder Metallurgy Steel using Artificial Neural Network. *Materials and Design* **2007**, 28, 2431-2442.
- [5] Umbrello, D.; Ambrogio, G.; Filice, L.; Shivpuri, R. A Hybrid Finite Element Method-Artificial Neural Network Approach for Predicting Residual Stresses and the Optimal Cutting Conditions during Hard Turning of AISI 52100 Bearing Steel. *Materials and Design* **2008**, 29, 873-883.
- [6] Coello Coello, C.A.; Becerra, R.L. Evolutionary Multiobjective Optimization in Materials Science and Engineering, *Materials and Manufacturing Processes* **2009**, 24(2), 119-129.
- [7] Zhang, Q.; Mahfouf, M. Fuzzy Predictive Modelling using Hierarchical Clustering and Multi-Objective Optimisation for Mechanical Properties of Alloy Steels. In *Proceedings of the 12th IFAC Symposium on Automation in Mining, Mineral and Metal Processing*, 2007, pp. 427-432.
- [8] Zhang, Q. Nature-Inspired Multi-Objective Optimisation and Transparent Knowledge Discovery via Hierarchical Fuzzy Modelling. PhD Thesis, The Department of Automatic Control and Systems Engineering, The University of Sheffield, UK, 2008.
- [9] Deb, K.; Pratap, A.; Agarwal, S.; Meyarivan, T. A Fast and Elitist Multiobjective Genetic Algorithm: NSGA-II. *IEEE Transactions on Evolutionary Computation* **2002**, 6 (2), 182-197.
- [10] Sim, W.M. Challenges of Residual Stress and Part Distortion in the Civil Airframe Industry. In *Proceedings of the 2nd International Conference on Distortion Engineering*, 2008.
- [11] Denkena, B.; Boehnke, D.; de Leon, L. Machining Induced Residual Stress in Structural Aluminum Parts, *Production Engineering* **2008**, 2(3), 247-253.
- [12] Boumaiza, S.; Pinna, C.; Yates, J.R.; Greene, R.J. Finite Element Modelling of Part Distortion under Residual Stress, to be submitted.

- [13] Wang, L.-X.; Mendel, J.M. Fuzzy Basis Functions, Universal Approximation, and Orthogonal Least-squares Learning, *IEEE Transactions on Neural Networks* **1992**, 3 (5), 807-814.
- [14] Wang, L.-X.; *A Course in Fuzzy Systems and Control*. Prentice-Hall: Englewood Cliffs, NJ, USA, 1997.
- [15] Zhang, Q.; Mahfouf, M. Mamdani-Type Fuzzy Modelling via Hierarchical Clustering and Multi-Objective Particle Swarm Optimisation (FM-HCPSO). *International Journal of Computational Intelligence Research (IJCIR)* **2008**, 4 (4), 314-328.
- [16] Ishibuchi, H.; Nojima, Y. Analysis of Interpretability-accuracy Tradeoff of Fuzzy Systems by Multiobjective Fuzzy Genetics-based Machine Learning. *International Journal of Approximate Reasoning* **2007**, 44 (1), 4-31.
- [17] Alcalá, R.; Ducange, P.; Herrera, F.; Lazzerini, B.; Marcelloni, F. A Multiobjective Evolutionary Approach to Concurrently Learn Rule and Data Bases of Linguistic Fuzzy-rule-based Systems. *IEEE Transactions on Fuzzy Systems* **2009**, 17 (5), 1106-1122.
- [18] Withers, P.J.; Bhadeshia, H.K.D.H. Residual Stress Part 1 - Measurement Techniques. *Materials Science and Technology* **2001**, 17, 355-365.
- [19] Koc, M.; Culp, J.; Altan, T. Prediction of Residual Stresses in Quenched Aluminium Blocks and Their Reduction through Cold Working Processes. *Journal of Materials Processing Technology* **2006**, 174, 342-354.
- [20] Jackiewicz, J. Assessing Coefficients of the Barlat Yield Criterion for Anisotropic Aluminum Alloy Sheets by Means of the Evolutionary Strategy. *Materials and Manufacturing Processes* **2009**, 24 (3), 375-383.
- [21] Zhang, Q.; Mahfouf, M. A Modified PSO with a Dynamically Varying Population and Its Application to the Multi-Objective Optimal Design of Alloy Steels. In *Proceedings of the 2009 IEEE Congress on Evolutionary Computation*, 2009, pp. 3241-3248.
- [22] Paszkowicz, W. Genetic Algorithms, a Nature-Inspired Tool: Survey of Applications in Materials Science and Related Fields. *Materials and Manufacturing Processes* **2009**, 24 (2), 174-197.
- [23] Zadeh, L.A. A Fuzzy-set-theoretic Interpretation of Linguistic Hedges. *Journal of Cybernetics* **1972**, 2, 4-34.
- [24] Mahfouf, M.; Gama, M.A.; Panoutsos, G. "Right-First-Time" Production: a Reality or a Myth? *Materials and Manufacturing Processes* **2009**, 24 (1), 78-82.
- [25] Zhang, Q.; Mahfouf, M. A Nature-Inspired Multi-Objective Optimisation Strategy Based on a New Reduced Space Searching Algorithm - Special Application to the Design of Alloy Steels. *Engineering Applications of Artificial Intelligence* **2010**, 23, 660-675.
- [26] Egorov-Yegorov, I.N.; Dulikravich, G.S. Chemical Composition Design of Superalloys for Maximum Stress, Temperature, and Time-to-rupture using Self-adapting Response Surface Optimization. *Materials and Manufacturing Processes* **2005**, 20 (3), 569-590.
- [27] Dulikravich, G.S.; Egorov, I.N.; Colaco, M.J. Optimizing Chemistry of Bulk

- Metallic Glasses for Improved the Thermal Stability. Modelling and Simulation in Materials Science and Engineering **2008**, 16 (7), 075010.
- [28] Dieter, G.E. Mechanical Metallurgy: SI metric edition, McGraw-Hill: London, 1988.

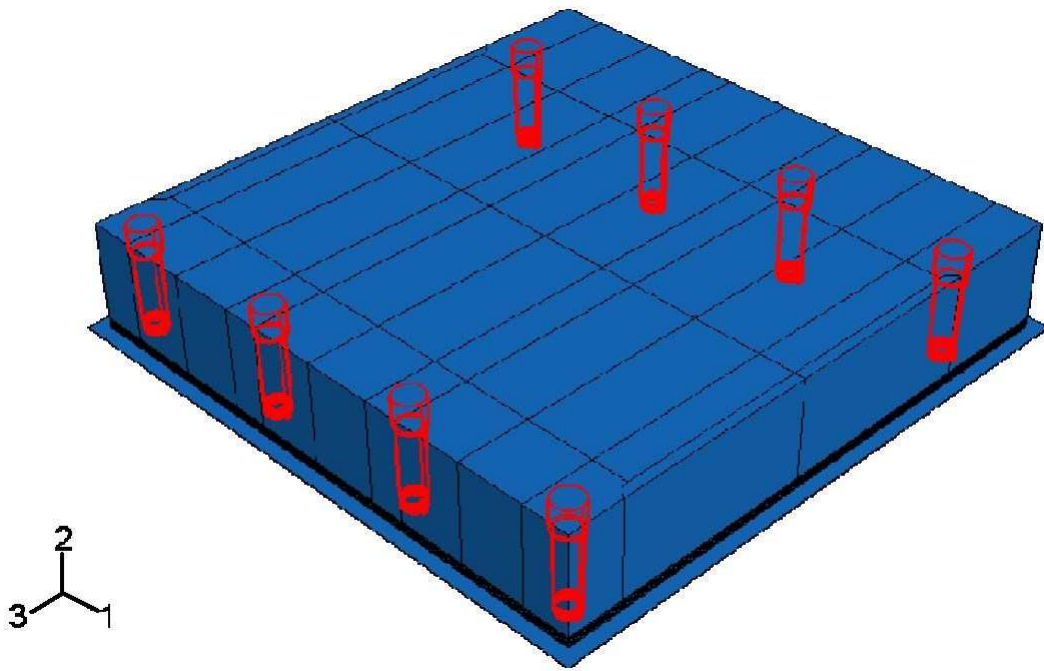


Figure 1. The initial geometry of a specimen with clamping holes

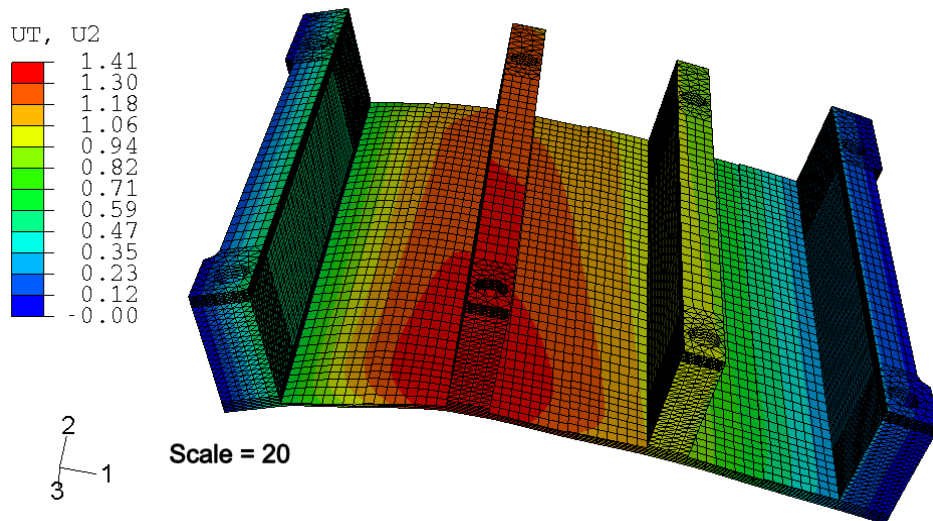


Figure 2. Final distortion of the machined component

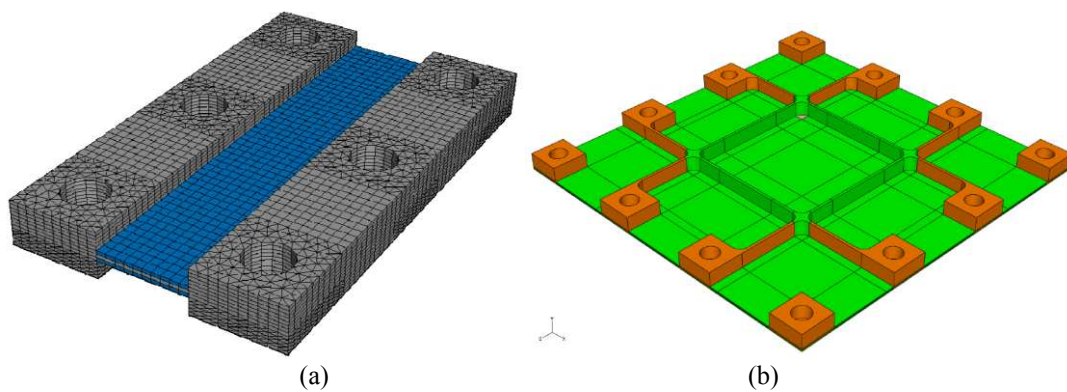


Figure 3. Geometry of two machined specimens: (a) a single channel specimen machined from both sides and (b) a nine-pocket specimen

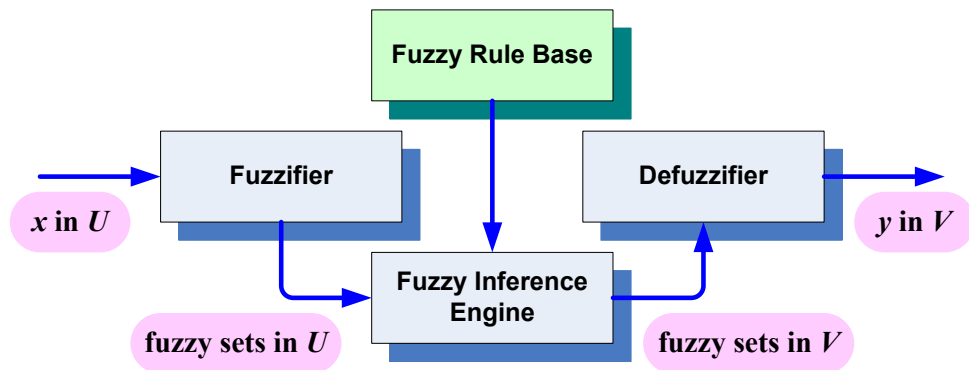


Figure 4. Basic configuration of fuzzy systems

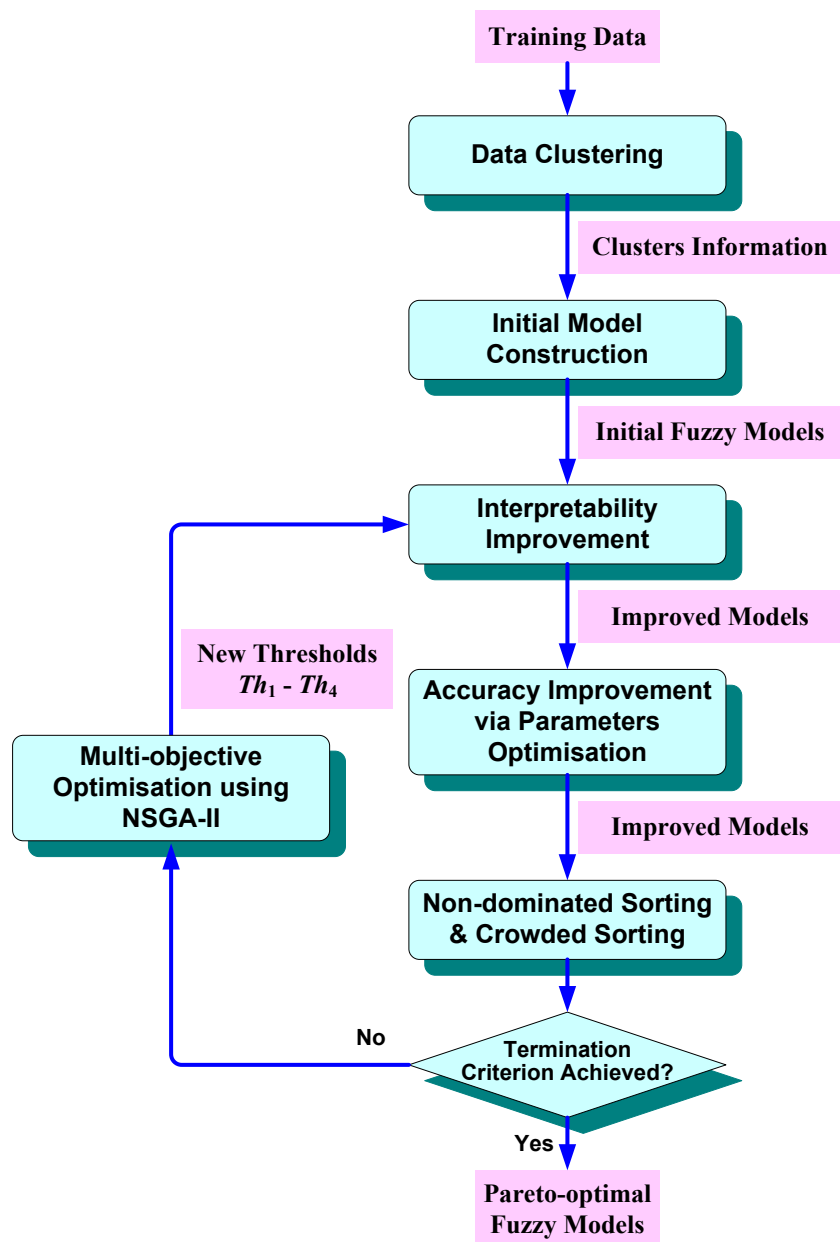


Figure 5. The flow chart of the proposed fuzzy modelling approach

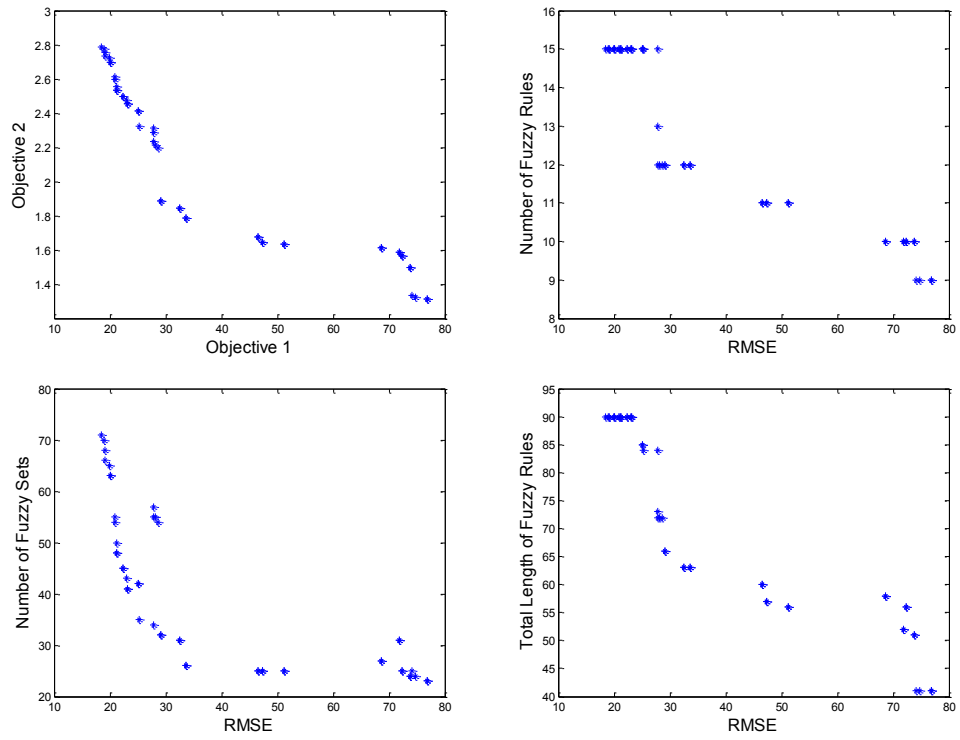


Figure 6. The performance of one set of optimised Pareto-optimal fuzzy models for the 5-dimensional residual stress modelling problem

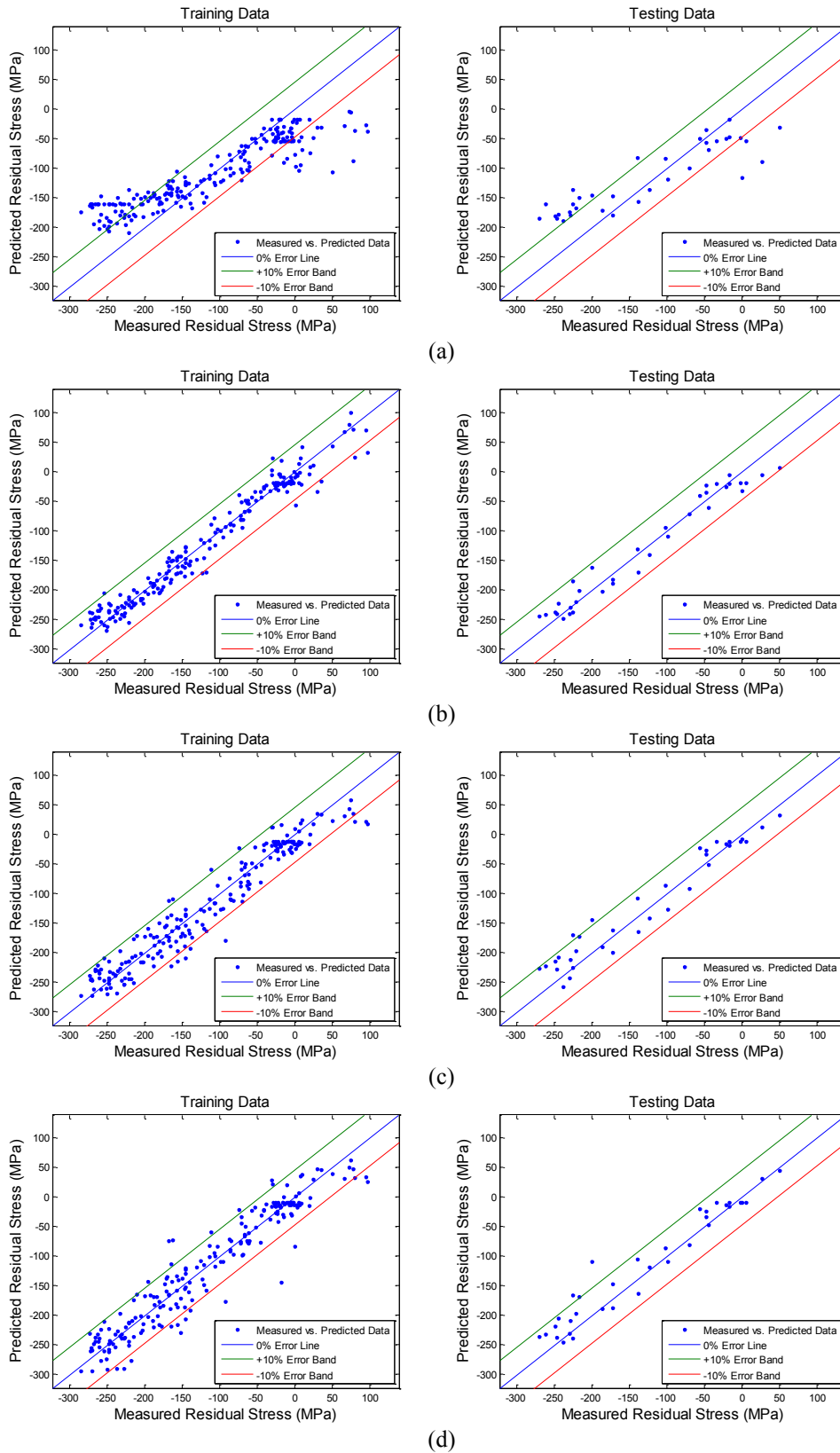


Figure 7. The residual stress models' predicted outputs versus measured outputs: (a) the initial model, (b) an optimised model with 15 rules, (c) an optimised model with 14 rules, and (d) an optimised model with 12 rules; the green and red lines represent the +10% and -10% error bands respectively

R_5

R_{14}

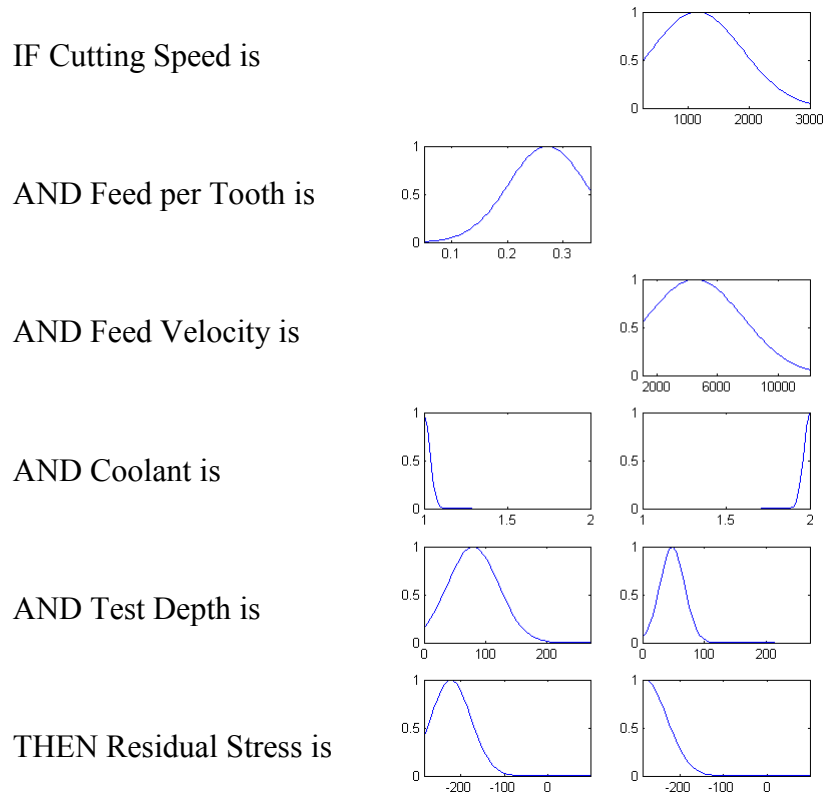


Figure 8. Two fuzzy rules of the optimised 14-rule residual stress model

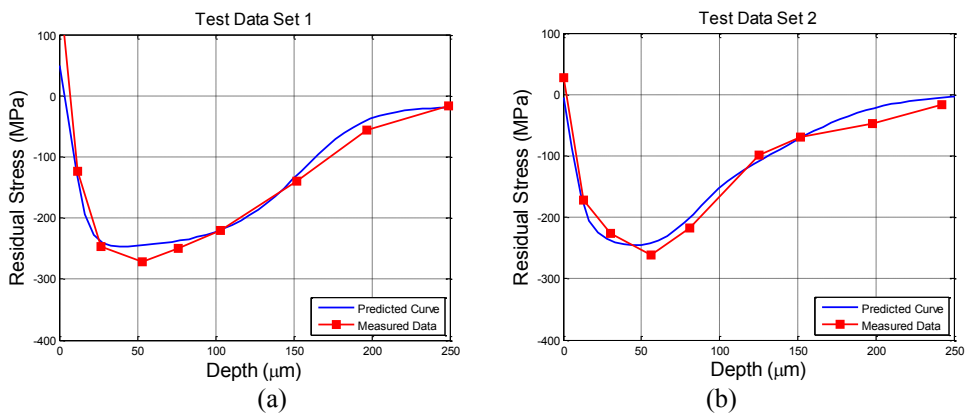


Figure 9. Comparison between the optimised 15-rule model's predicted residual stress curve and the measured residual stress curve: (a) test data set 1 and (b) test data set 2

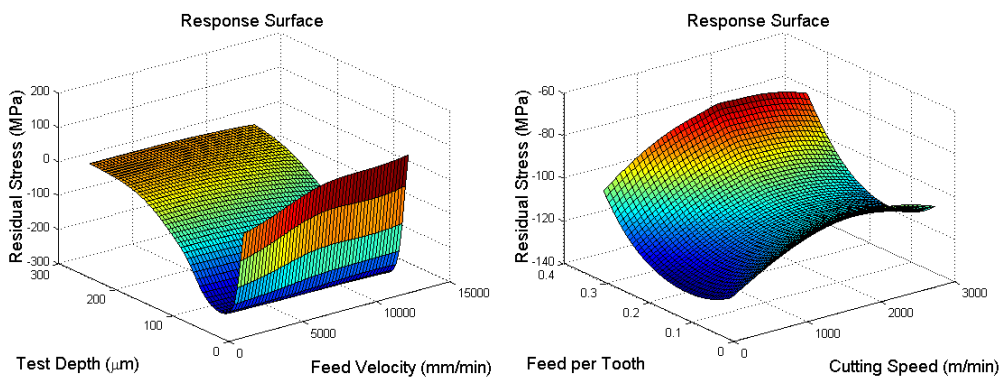


Figure 10. Response surfaces of the optimised 15-rule residual stress model

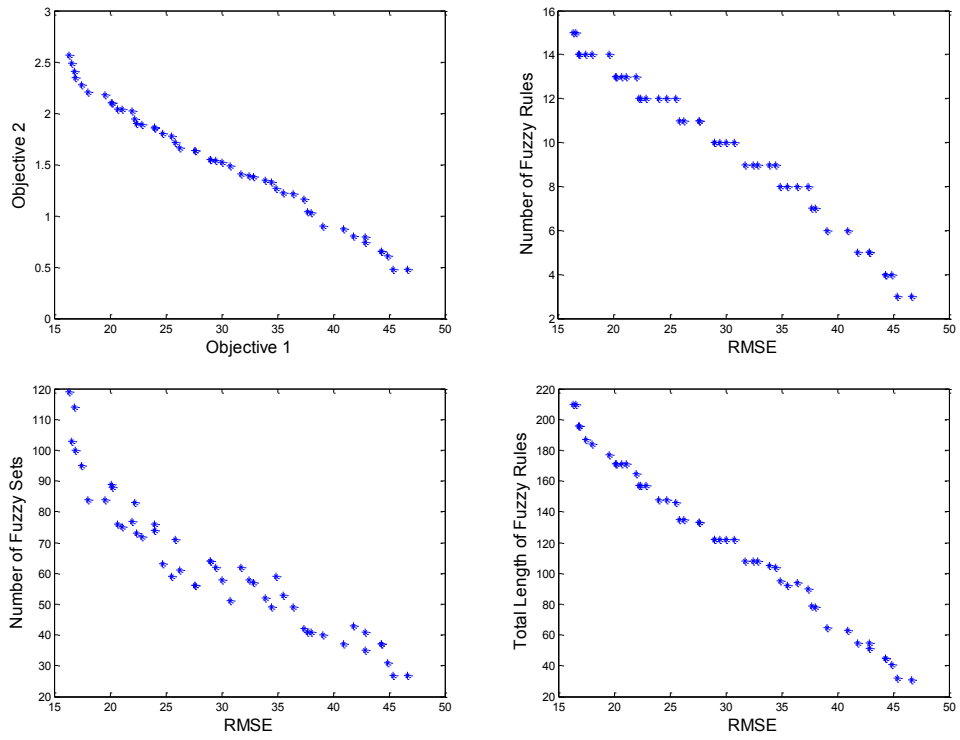


Figure 11. The performance of one set of optimised Pareto-optimal fuzzy models for the 13-dimensional residual stress modelling problem

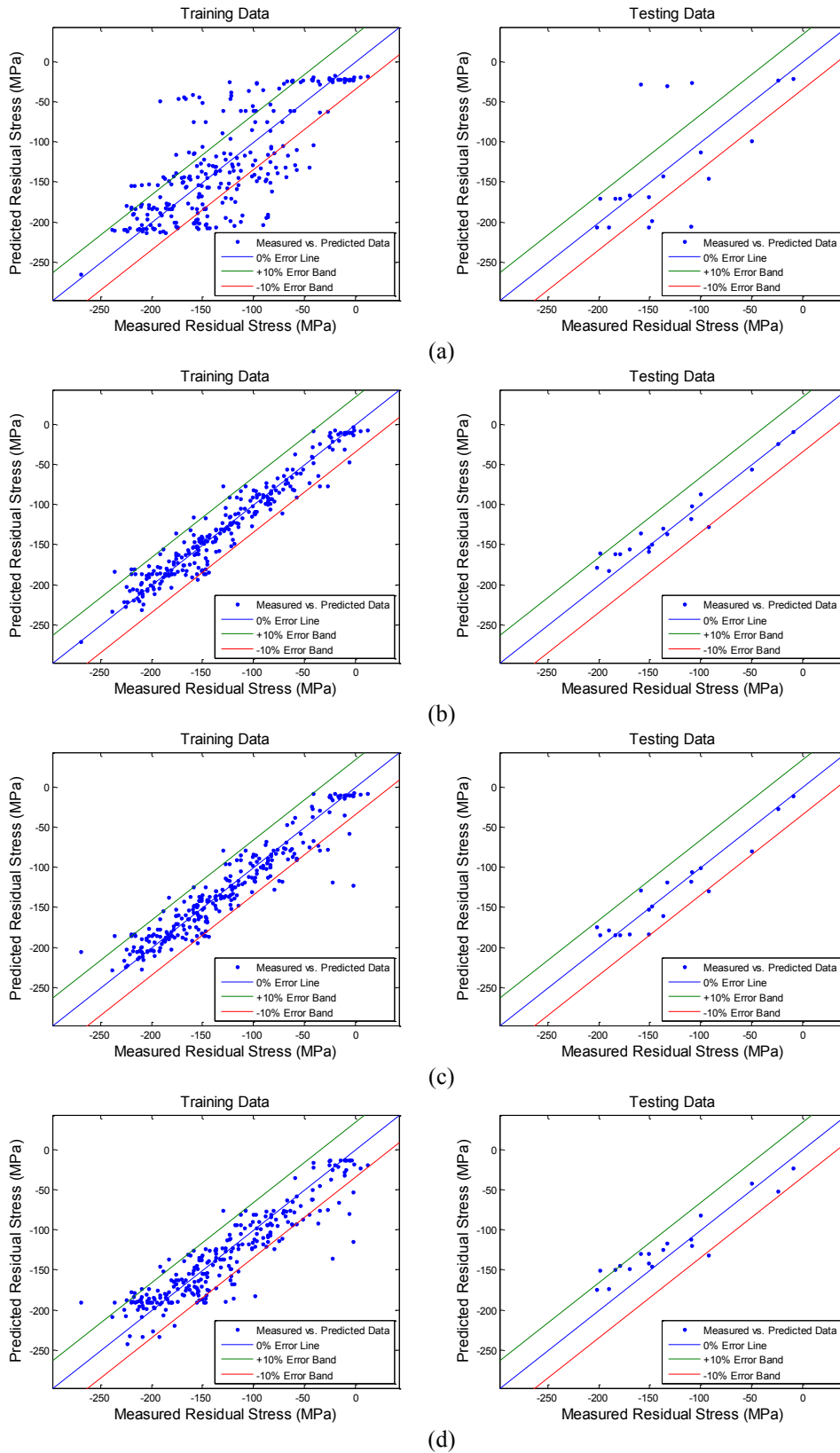


Figure 12. The residual stress models' predicted outputs versus measured outputs: (a) the initial model, (b) an optimised model with 15 rules, (c) an optimised model with 13 rules, and (d) an optimised model with 12 rules; the green and red lines represent the +10% and -10% error bands respectively

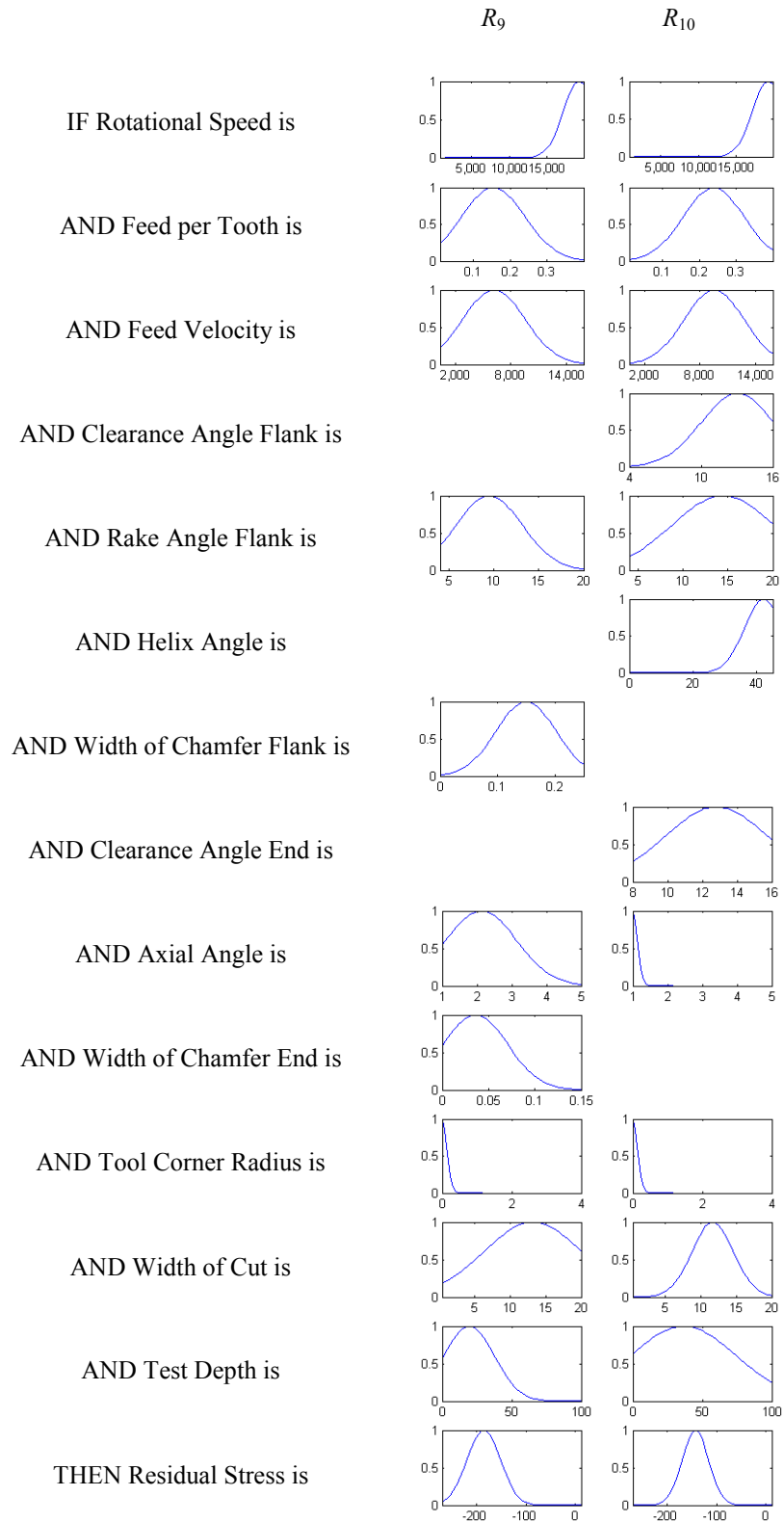


Figure 13. Two fuzzy rules of the optimised 13-rule residual stress model

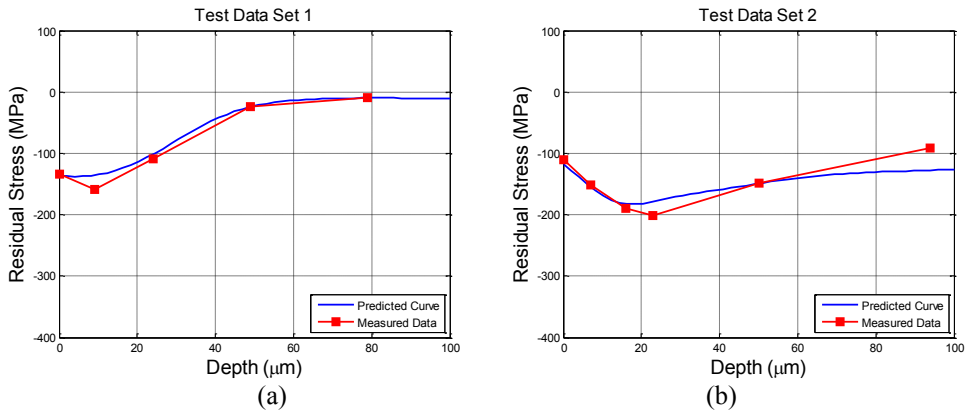


Figure 14. Comparison between the optimised 15-rule model's predicted residual stress curve and the measured residual stress curve: (a) test data set 1 and (b) test data set 2

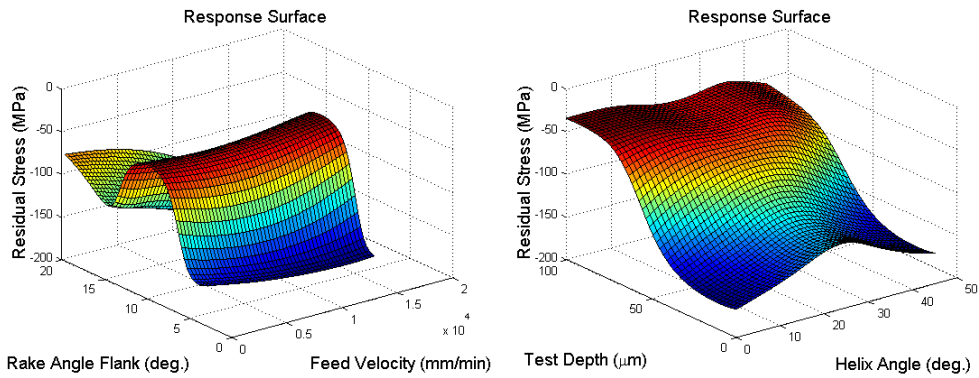


Figure 15. Response surfaces of the optimised 15-rule residual stress model

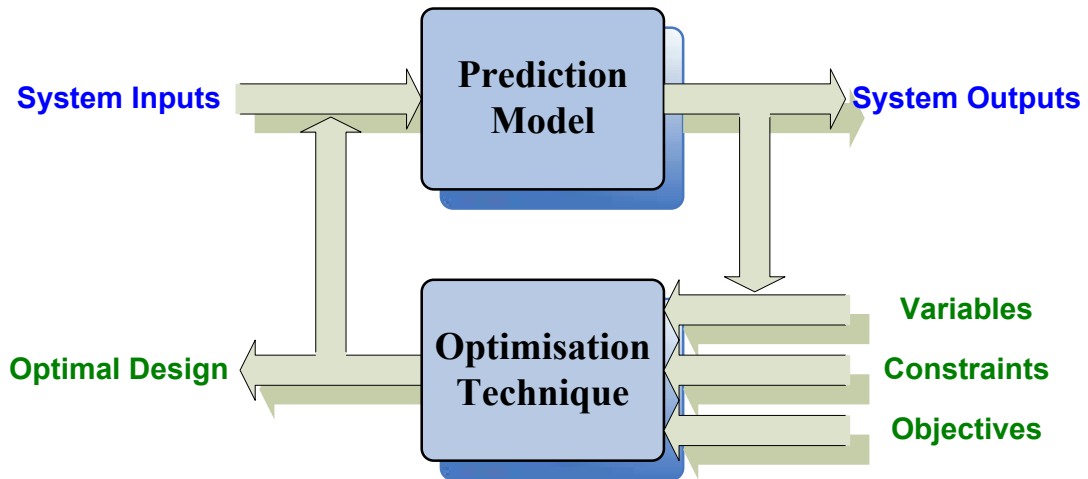


Figure 16. Optimal machining process design via reverse-engineering

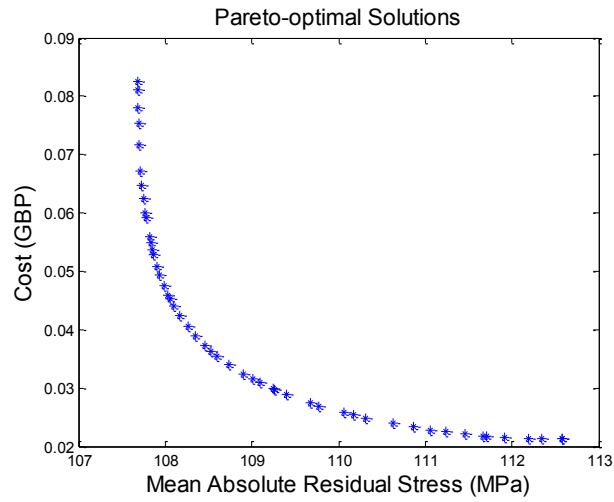


Figure 17. The performance of one set of Pareto-optimal solutions for the first optimal design problem

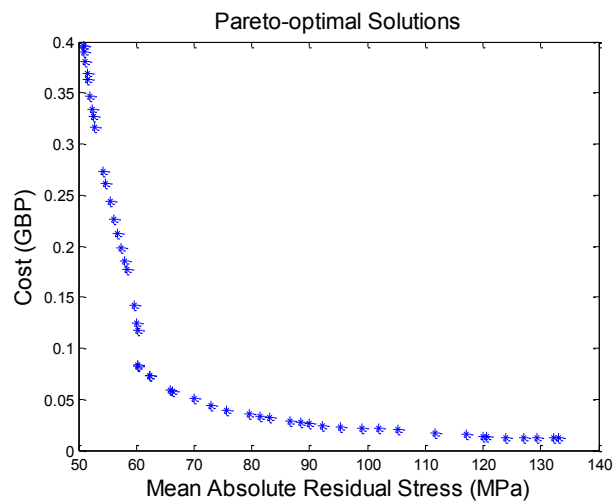


Figure 18. The performance of one set of Pareto-optimal solutions for the second optimal design problem

Table 1. Main parameters of some obtained residual stress models

| Fuzzy model | Number of fuzzy sets for each variable | Rule length of each fuzzy rule | RMSE of all the training data | RMSE of the testing data |
|-------------------------------|--|---|-------------------------------|--------------------------|
| Initial model with 15 rules | Inputs: [15; 15; 15; 15; 15] Output: 15 | [5; 5; 5; 5; 5; 5; 5; 5; 5; 5; 5; 5; 5; 5; 5] | 52.98 | 65.35 |
| Optimised model with 15 rules | Inputs: [14; 15; 14; 3; 12] Output: 12 | [5; 5; 5; 5; 5; 5; 5; 5; 5; 5; 5; 5; 5; 5; 5] | 18.89 | 29.16 |
| Optimised model with 14 rules | Inputs: [8; 6; 7; 2; 6] Output: 6 | [5; 5; 5; 3; 3; 5; 5; 4; 5; 5; 5; 5; 5; 5; 4] | 25.21 | 35.57 |
| Optimised model with 12 rules | Inputs: [7; 5; 6; 2; 6] Output: 6 | [5; 5; 3; 3; 5; 5; 4; 5; 5; 5; 5; 5; 4] | 29.12 | 35.66 |

Table 2. Main parameters of some obtained residual stress models

| Fuzzy model | Number of fuzzy sets for each variable | Rule length of each fuzzy rule | RMSE of all the training data | RMSE of the testing data |
|-------------------------------|--|--|-------------------------------|--------------------------|
| Initial model with 15 rules | Inputs: [15; 15; 15; 15; 15; 15; 15; 15; 15; 15; 15; 15; 15; 15; 15] Output: 15 | [13; 13; 13; 13; 13; 13; 13; 13; 13; 13; 13; 13; 13; 13; 13] | 42.93 | 54.48 |
| Optimised model with 15 rules | Inputs: [6; 9; 9; 6; 7; 7; 6; 6; 5; 5; 3; 8; 12] Output: 14 | [13; 13; 13; 13; 13; 13; 13; 13; 13; 13; 13; 13; 13; 13; 13] | 16.53 | 16.83 |
| Optimised model with 13 rules | Inputs: [4; 6; 7; 4; 4; 5; 5; 4; 4; 4; 3; 7; 8] Output: 11 | [13; 13; 12; 11; 13; 12; 12; 13; 10; 11; 13; 13; 12] | 20.73 | 18.44 |
| Optimised model with 12 rules | Inputs: [4; 5; 7; 3; 3; 4; 5; 3; 3; 4; 2; 5; 6] Output: 5 | [13; 13; 12; 10; 13; 9; 11; 12; 9; 8; 12; 12] | 25.56 | 24.21 |

Table 3. Parameter values for the machining cost

| Parameter | K_L (£/min) | L (mm) | K_T (£) | K | n |
|-----------|---------------|----------|-----------|------|------|
| Value | 1 | 100 | 2000 | 5544 | 0.15 |

Table 4. Ten of the Pareto-optimal solutions for the first optimal design problem

| Solutions | 1 | 2 | 3 | 4 | 5 | 6 | 7 | 8 | 9 | 10 |
|-------------------------------------|--------|--------|--------|--------|--------|--------|--------|--------|--------|--------|
| Cutting speed (m/min) | 316.87 | 396.28 | 461.43 | 538.93 | 635.21 | 764.66 | 861.40 | 1019.7 | 1201.9 | 1333.0 |
| Feed velocity (mm/min) | 1281.5 | 1602.6 | 1866.1 | 2179.5 | 2568.9 | 3092.3 | 3483.6 | 4123.6 | 4860.7 | 5390.8 |
| Mean Absolute Residual Stress (MPa) | 107.69 | 107.75 | 107.85 | 108.04 | 108.35 | 108.90 | 109.39 | 110.31 | 111.46 | 112.34 |
| Machining cost (£) | 0.0780 | 0.0624 | 0.0536 | 0.0459 | 0.0390 | 0.0325 | 0.0289 | 0.0249 | 0.0221 | 0.0213 |

Table 5. Ten of the Pareto-optimal solutions for the second optimal design problem

| Solutions | 1 | 2 | 3 | 4 | 5 | 6 | 7 | 8 | 9 | 10 |
|-------------------------------------|------------|------------|------------|------------|------------|------------|------------|------------|-----------------|-----------------|
| Cutting speed (m/min) | 253.93 | 250.00 | 250.04 | 250.08 | 250.00 | 344.41 | 527.90 | 757.31 | 1325.8 | 1340.4 |
| Feed per tooth | 0.0500 | 0.0593 | 0.0810 | 0.1118 | 0.2403 | 0.2828 | 0.2912 | 0.2805 | 0.3057 | 0.3500 |
| Feed velocity (mm/min) | 256.72 | 299.73 | 409.43 | 565.30 | 1214.7 | 1969.2 | 3107.9 | 4295.6 | 8195.1 | 9485.7 |
| Coolant medium | <i>dry</i> | <i>dry</i> | <i>dry</i> | <i>dry</i> | <i>dry</i> | <i>dry</i> | <i>dry</i> | <i>dry</i> | <i>emulsion</i> | <i>emulsion</i> |
| Mean Absolute Residual Stress (MPa) | 51.016 | 52.377 | 55.405 | 58.341 | 60.312 | 70.052 | 83.136 | 95.251 | 120.00 | 129.35 |
| Machining cost (£) | 0.3895 | 0.3336 | 0.2442 | 0.1769 | 0.0823 | 0.0508 | 0.0322 | 0.0234 | 0.0140 | 0.0122 |